the weight parameters, shown in Table 3, were used for the aeroprecursor system.

Figure 9 suggests an answer to the question whether precursors are necessary if "adequate atmospheric information is available." It is not difficult to postulate a future time period in which uncertainties in our knowledge of the Martian atmosphere are possibly reduced to the point where the atmosphere can be used for braking purposes without data augmentation. However, the desirability, as opposed to the necessity, of incorporating precursors should be considered. Uncertainties in the knowledge of the atmosphere will still remain, and the propulsive requirements to attain the prescribed orbit after the atmospheric flight are a strong function of these uncertainties. Significant increases in payload can also result from reductions in these propulsive requirements, as may be inferred from Fig. 9.

Conclusions

The use of precursor vehicles to probe planetary atmospheres prior to the entry of a spacecraft appears to make possible the use of atmospheric braking in spite of substantial uncertainties in knowledge of the atmospheric characteristics. A feasibility study of the complete system indicates a very attractive potential for the concept; a more detailed design study seems warranted.

References

[1] Hohmann, W., "The attainability of the heavenly bodies," NASA TTF-44 (November 1960).

[2] Chapman, D., "An analysis of the corridor and guidance requirements for supercircular entry into planetary atmospheres," NASA TR R-55 (1960).

[3] Warga, J. and Hailey, W. C., "The determination of extreme entry angles into a planetary atmosphere," AIAA Preprint 63-152 (June 1963).

[4] Leon, H., "Spin dynamics of rockets and space vehicles in vacuum," Space Technology Lab. Inc., AD-229-739 (September 16, 1959).

[5] "Project Voyager status report, June-August, 1962," Avco Research and Development Div. RAD-TM-62-80 (October 16, 1962).

[6] Dow, P. C., Fields, D., and Scammell, F., "Automatic re-entry guidance at escape velocity," ARS Preprint 1946-61 (August 1961).

SEPTEMBER-OCTOBER 1964 J. SPACECRAFT VOL. 1, NO. 5

Hall-Current Accelerator Utilizing Surface Contact Ionization

EDWARD A. PINSLEY,* CLYDE O. BROWN,† AND CONRAD M. BANAS‡
United Aircraft Corporation, East Hartford, Conn.

Analyses and experiments were performed on a Hall-current accelerator in which ion acceleration occurs in an annular region filled with a neutral, fully ionized, nonequilibrium cesium plasma. Cesium ions are formed by both surface contact and volume ionization, and electrons are introduced by a downstream cathode. Acceleration is achieved by interaction of a radial magnetic field and an impressed axial electric field producing azimuthal electron drifts. Magnetic field strength is adjusted such that $\omega_e\tau_e \gg 1$, and the ion cyclotron radius is large compared with accelerator length. Accordingly, axial electron currents are inhibited by the magnetic field, whereas ion currents are unaffected. Constraints on accelerator performance and design imposed by the onset of a two-stream instability are considered. Losses due to this instability can be avoided by properly choosing operating variables and accelerator size. Efficient, high-thrust-density performance is theoretically achievable at moderate specific impulse with large accelerators and high thrust levels, provided that electron backflow can be held to tolerable limits. Potential advantages include high tolerance to neutral efflux and low ionizer heater requirements. Preliminary tests have been conducted on an experimental accelerator and ion source under conditions of exhaust beam current neutrality.

Introduction

USE of a low-density Hall-current accelerator to circumvent the space-charge-limited current operation of conventional ion accelerators has been suggested[1] as a means of obtaining high-performance electric propulsion thrustors in the moderate (2000–5000 sec) specific impulse regime. Neutralization of the ion space charge in this device is achieved by the introduction of an equal number density of electrons in an annular accelerating region. Electrons are constrained to azimuthal Hall-current drift motions by a radial magnetic field and an impressed axial electric field that also provides a means of adding directed kinetic energy to the ions. The Hall-current Lorentz force couples the ion reaction force to the accelerator structure. The accelerating region is filled with a low-density, collisionless ($\omega_e\tau_e \gg 1$) plasma, in which the ion cyclotron radius is large and the electron cyclotron radius is small with respect to accelerator dimensions. This so-called "EM-region" plasma, in principle, permits electrostatic acceleration of ions while electrons are constrained to $\mathbf{E} \times \mathbf{B}$ drift motions.

Previous experimental investigations[2–5] have been conducted on devices in which argon ions are formed by volume ionization in the accelerating region. To sustain the discharge it has been necessary to operate such accelerators at rather high neutral gas pressures (over 10^{-3} mm Hg). The presence of background neutrals at these pressures can de-

Presented as Preprint 64-23 at the AIAA Aerospace Sciences Meeting, New York, January 20–22, 1964; revision received June 4, 1964.

* Chief, Electrical Propulsion, Research Laboratories. Associate Fellow Member AIAA.

† Associate Research Engineer, Electrical Propulsion, Research Laboratories. Member AIAA.

‡ Research Engineer, Electrical Propulsion, Research Laboratories. Member AIAA.

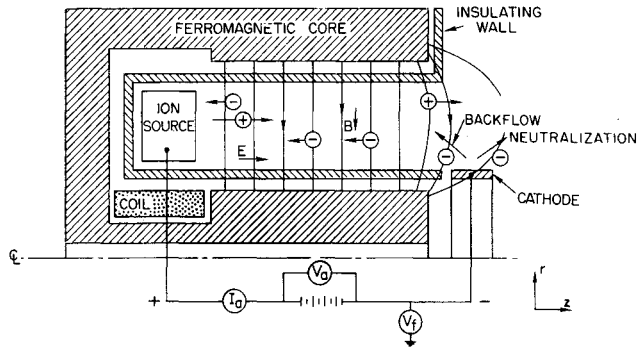

Fig. 1 Accelerator cross section.

crease collision times to the point where the plasma is collision dominated, causing appreciable losses due to increased axial electron currents. In addition, in such gas discharge devices, ions are formed at intermediate energies, giving rise to losses because of, first, the migration to the anode of electrons released in these ionizations, and second, beam nonuniformities and loss of ionized gas. To retain the desirable feature of space-charge neutralized ion acceleration and yet avoid the problems associated with the gas discharge device, consideration has been given to the design of a Hall-current accelerator that would employ cesium as a propellant, and that would provide for the generation of ions by surface contact ionization as well as volume ionization.

The purpose of the program described herein is to evaluate in a preliminary fashion the potentialities for electric propulsion purposes of an EM-region, Hall-current accelerator in which cesium is introduced into the accelerating region through a heated, porous tungsten surface. A number of problems relating to the operation of such a device can be examined analytically, at least in a qualitative sense. However, several questions regarding electron transport processes, the character of the discharge, and exhaust beam neutralization can best be answered by experiment. Accordingly, an experimental program was undertaken, and preliminary results are described herein.

Description of Ion Acceleration Process

The plasma regime of interest in the present Hall-current accelerator is one of relatively low electron energy ($\sim$100 ev) and consequently low magnetic field strength ($\lesssim$1000 gauss). To prevent the formation of Hall potentials, an annular geometry is employed, resulting in a short-circuited Hall current. These factors suggest the use of a solenoid coil and ferromagnetic core arrangement (Fig. 1), which provides a relatively uniform magnetic field throughout the accelerating region. The classical mobility of electrons within the accelerating region is reduced by the presence of the radial magnetic field, provided the condition $\omega_b \gg \nu_c$ is satisfied. These electrons provide the neutralizing space charge for ions that are accelerated by an axial electric field maintained within the plasma. Insulating walls prevent the magnet pole pieces from short circuiting this electric field. Electrons for space charge neutralization in the accelerating region are emitted from the same cathode that provides electrons for beam current neutralization. A thermionic cathode that can be shielded from ion interception by the accelerator structure provides a convenient electron source. As shown in Fig. 1, the magnetic field lines can be arranged to pass through the cathode and guide electrons into the beam region. For efficient operation of the accelerator, it is necessary that the electron backflow current J_{ez}, required to provide space-charge neutralization in the accelerator, be small compared to the current required for beam neutralization $J_{ez} < J_{eB} = J_i$. The total current I_a through the accelerator power supply comprises contributions from J_{ez} and J_{eB}.

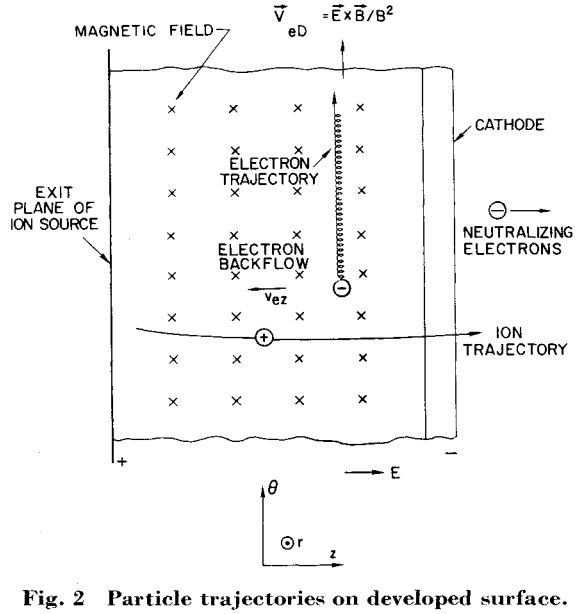

Fig. 2 Particle trajectories on developed surface.

Particle trajectories projected on a cylindrical surface within the accelerating region are shown, on a development of this surface, in Fig. 2. Electron trajectories are comprised of a circular thermal motion added to an azimuthal $\mathbf{E} \times \mathbf{B}$ drift, giving the trajectories shown. Even infrequent collisions can cause local electron thermalization and introduce radial electron motions. However, annular wall losses are minimized by the presence of radial electric fields in narrow wall sheath regions which result from the insulator surface charge (provided that the secondary emission coefficient of the wall is less than 1). Since the net local current to the insulating wall is zero, losses are thus a function of radial ion currents which can be reduced to small values by proper accelerator design. Ion motions are governed primarily by the axial electric field, and, as shown in Fig. 2, ion trajectories are unaffected by the presence of the relatively low radial magnetic field. With a surface contact ion source, ions formed on the surface have essentially the same energies and trajectories; those formed by electron impact ionization of neutrals in the accelerating region will have an energy distribution.

An approximate description of the behavior of the accelerator can be obtained by considering the macroscopic equations of motion of each species,

$$nq_s\mathbf{E} + \mathbf{J}_s \times \mathbf{B} - \nabla p_s - nq_s\eta\mathbf{J} = m_s n(D\mathbf{v}_s/Dt) \quad (1)$$

where $n = n_e \approx n_i$, and η is a scalar resistivity. For the ions, under the condition $E_\theta = E_r = 0$, this reduces to

$$E_z - \eta J_z = (m_i/e)dv_{iz}/dt$$

which indicates that the ions are accelerated by a force produced by the electric field less a drag introduced by electron-ion collisions. Since such collisions are infrequent and are not effective in transferring momentum, the second term may be neglected compared to the first, and

$$m_i v_i^2/2 = eV_a - eV(z)$$

where V_a is the ionizer potential. This is the usual result for electrostatic engines and indicates that for efficient operation the exhaust beam potential should approach the neutralizer (in this case the cathode) potential.

For the electrons, the right side of Eq. (1) may be neglected in the absence of accelerated axial drift. The geometry of the device permits us to set $E_\theta = E_r = B_\theta = B_z = 0$. In addition, since we are dealing with an essentially collisionless plasma, we neglect electron pressure gradients in comparison to the remaining terms in Eq. (1). This, in essence, is equivalent to the assumption that energy transport is convective

rather than conductive and allows us to circumvent, for the moment, the need for determining a local electron temperature (or average energy in the absence of electron thermalization). The determination of the electron temperature distribution would entail consideration of the axial energy transport process and would require the introduction of two additional transport coefficients. Furthermore, the assumption is conservative in the sense that the presence of axial diffusion would apparently inhibit electron backflow. Accordingly, for electron momentum in the axial and azimuthal directions

$$neE_z + J_{e\theta}B_r = \mu_z m_e J_z/e \tag{2}$$

and

$$J_{ez}B_r = -\nu_c m_e J_{e\theta}/e \tag{3}$$

where $J_z = J_i + J_{ez}$ and where ν_c is an "effective" momentum-loss collision frequency.[6] Equations (2) and (3) yield

$$J_{ez}/J_{e\theta} = -\nu_c/\omega_b \tag{4}$$

and

$$E_z = -dV/dz = \frac{J_{ez}m_e\nu_c}{ne^2}\left[1 + \frac{J_i}{J_{ez}} + \left(\frac{\omega_b}{\nu_c}\right)^2\right] \tag{5}$$

where ω_b is the electron cyclotron frequency. As shown in Ref. 1, Eq. (4) requires that $\omega_b \gg \nu_c$ for small J_{ez} and hence for efficient accelerator performance.

The solution of Eq. (5) is complicated by several factors. First, if appreciable volume ionization occurs (as is the case in the gas discharge type of Hall accelerator) both J_{ez} and J_i vary with axial position in a manner determined by neutral gas density, electron density, and electron energy distribution. In the case of the surface contact ionization, however, J_i, and hence J_{ez}, are nearly constant with z, except for a small contribution due to the ionization of the residual neutral efflux. Second, to determine a suitably averaged value of ν_c, it is necessary to know the local electron temperature, or, in the absence of electron thermalization, the local velocity distribution. If, as assumed previously, energy transport is a primarily convective process, and if energy losses to the annulus walls and to the ions are small, the temperature at any axial position will be determined by the potential at that position. Since $n_e \approx n_i = (J_i/e)[2e(V_a - V)/m_i]^{-1/2}$, with appropriate assumptions regarding neutral densities and various particle-particle collision processes, it is possible, in the case of classical electron transport, to integrate Eq. (5). This would determine the impedance of the accelerating region to electron backflow, as well as the axial potential distribution. However, in low-pressure discharges, diffusion across magnetic fields can occur at enhanced or "anomalous" rates which are considerably in excess of values predicted by classical theory.[7] Both macroscopic and microscopic instabilities can contribute to such enhanced transport processes. The extent to which these instabilities contribute to an "effective" collision frequency ν_c in the low-density Hall-current accelerator environment is not presently known; this effect can best be determined by experiment. Some recent work[6] has suggested the presence of two-stream instabilities at electric fields above a critical value. Means of avoiding this condition and the effect on accelerator design are discussed later.

The form of Eq. (5) implies that for $\omega_b \gg \nu_c$ and for the region of interest of electron backflow, $J_{ez} \lesssim 0(J_i)$, the product $J_{ez}L$ (where L is the accelerator length) is a function of V_a, B, J_i and neutral density (for classical electron mobility). This implies that lengthening the accelerating region causes a corresponding increase in impedance to electron backflow with a resulting increase in efficiency. The condition that $r_i \gg L$, where r_i is the ion cyclotron radius, places an upper limit on accelerator length for a given ion exit velocity.

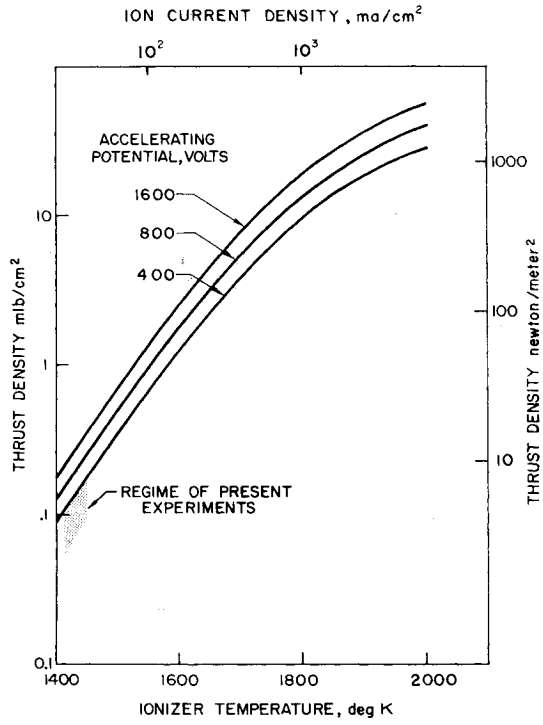

Fig. 3 Theoretical thrust density.

Ion Production

Ion production by surface contact ionization involves heating a high-work-function surface to emission temperatures (generally over 1400 K) and transporting cesium neutrals to the emitting surface. A porous ionizer was selected for the present study, although the Hall accelerator is quite adaptable to other configurations (e.g., a reverse-feed ionizer) which may offer distinct performance advantages.

Thermal radiation from the ionizer surface represents a major parasitic loss in the surface-contact device, as in the case of a conventional surface-contact ion engine. To reduce this loss to a small fraction of the over-all power input, it is necessary to operate at high power densities. In conventional ion engines which operate under space-charge-limited conditions, this is accomplished by operating at high net accelerating voltages, which increases specific impulse levels to values in the neighborhood of 5000 sec and above. With removal of space-charge current limitations, operation at low voltage (hence moderate specific impulse) is feasible provided that ion current densities can be increased to the order of 100 ma/cm.^{2} For both solid[8] and porous[9] surfaces, ion emission current density increases exponentially with temperature; however, radiated power increases as the fourth power of temperature. Hence, as ion current density is increased, efficiency also increases. Furthermore, it is possible to operate at relatively high thrust densities at these increased current levels. Using the ion emission current data of Ref. 8, theoretical thrust density has been computed for the surface-contact device and is presented in Fig. 3 as a function of ionizer temperature and accelerating voltage. Thrust densities considerably higher than values representative of present ion engines can be obtained at ionizer temperatures in the neighborhood of 1600 K in the specific impulse range of 2000–4000 sec.

The loss of un-ionized neutrals at high current densities is a serious problem for conventional electrostatic accelerators, principally because of electrode erosion due to sputtering by ions formed in charge exchange processes in the interelectrode region. In the Hall accelerator, however, the structure exposed to ion bombardment consists of insulating walls which can be constructed of alumina, for example, which has

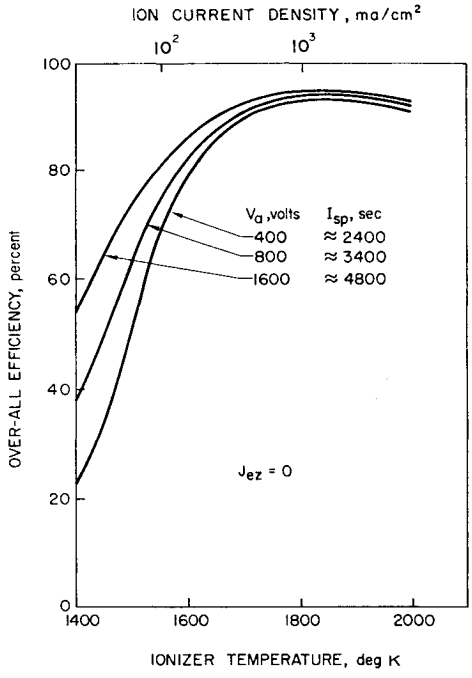

Fig. 4 Theoretical over-all efficiency.

excellent resistance to ion bombardment damage. Furthermore the alignment of these insulating surfaces is not critical to proper accelerator operation. Hence the existence of a large neutral fraction is not serious except in terms of increasing ν_c and reducing utilization efficiency. However, recently published data on the ionization cross section of cesium[10] indicate that, for the electron energy range of interest, the ionization cross section is quite large ($\sim 10^{14}$ cm^2), and hence essentially all neutrals will be ionized before leaving the vicinity of the ionizer. In the Hall-current accelerator, volume ionization thus effectively eliminates the problem of high neutral efflux at high ion current densities. In fact, it may ultimately prove desirable to design for operation with appreciable volume ionization in the vicinity of the ionizer as a means of introducing low-energy electrons into this region of high ion density.

Idealized Performance Analysis

The performance of the annular Hall accelerator is calculated to illustrate its suitability for use as an electrical propulsion thrustor and to evaluate the relative significance of the major losses on over-all efficiency in various operating regimes.

Sources of Loss

Assumptions regarding the various loss processes and the manner in which they have been included into the idealized performance analysis are given in the following paragraphs.

Electron backflow: This is the major loss present and the most difficult to estimate. Under the assumptions that insulating walls can be provided with a secondary emission coefficient less than one, and that ion wall interception currents will be small, the electron backflow will be essentially adiabatic. The backflow will thus dissipate the majority of its energy by electron bombardment at the ionizer surface, thereby reducing, and under conditions of high current density, eliminating completely ionizer heating power requirements. In the following performance analysis, over-all efficiency is calculated at various arbitrary values of J_{ez}/J_i under the assumption that losses due to backflow appear as thermal energy at the ionizer and that this energy is equally effective as the heater input in maintaining the ionizer at its operating temperature.

Ionizer radiation: Thermal radiation from the ionizer surface can be calculated if the temperature, the emissivity, and the heater effectiveness (to account for shielding, conduction losses, and edge effects) are known. In the following analysis the surface emissivity is taken as 0.4, and 50% of the heater input power is assumed to be lost due to back radiation, conduction, and edge effects.

Solenoid power: This factor will in all cases be small and is neglected in view of the possibility of using permanent magnet cores.

Wall losses: These losses are neglected in the idealized analysis. It should be possible to minimize wall losses by designing an accelerator having an annulus height approximately equal to the length of the accelerating region.

Neutralizer power: This loss is neglected in comparison to the ionizer power in the present analysis. Since the cathode can be shielded geometrically from high-energy ion bombardment it may prove feasible to use a low-work-function emitting material as the cathode.

Ion and neutral heating: The transfer of energy between electrons and heavy particles is relatively inefficient, and hence this source of loss is neglected. However, a small increase in ion thermal energy can be quite beneficial, as will be shown later, in increasing the critical electric field for avoiding the onset of two-stream instabilities.

Ion swirl: The azimuthal acceleration of ions due to the Lorentz force J_iB_r and the electron drag [right-hand side of Eq. (3)] can result in losses due to ion swirl (which appear in the form of exit-velocity spread and wall losses). However, under the conditions $L \ll r_i$ and $\omega_b \gg \nu_c$, where ν_c is now due only to particle-particle collisions, this effect is small.

Neutral efflux: This effect could be significant if no volume ionization occurs, or if charge exchange reactions occur in the vicinity of the ionizer surface and relatively fast neutrals are lost. Accordingly, in the following analysis, the neutral fraction leaving the ionizer is considered to cause a corresponding reduction in over-all efficiency.

Theoretical Efficiency

The significant loss processes are considered to consist of ionizer radiation, neutral efflux, and electron backflow. To evaluate the potentialities of the idealized surface-contact Hall accelerator, over-all efficiency ($\eta = F^2/2\dot{m}P$) is calculated as a function of ionizer temperature and accelerating voltage, first assuming $J_{ez} = 0$. Ion emission current and neutral efflux data were taken for solid tungsten from Ref. 8, which is optimistic by perhaps a factor of 2 for porous surfaces[9] but is offset somewhat by the assumption of no volume ionization. The results, presented in Fig. 4, indicate that efficiencies in excess of 50% can be obtained at ionizer temperatures in excess of 1500 K in the moderate specific impulse regime.

The effect of electron backflow is shown in Fig. 5 for $V_a = 800$ v. It is to be noted that at low ionizer temperatures (low ion current densities) the over-all efficiency is not affected by electron backflow because of the reduction in ionizer heater input requirements by an amount equal to $J_{ez}V_a$. At high ionizer temperatures (high ion current densities) bombardment due to electron backflow can completely eliminate the need for ionizer heater power. From Fig. 5, it can be seen that even at values of J_{ez}/J_i as high as 0.5 reasonable efficiencies can be obtained. Furthermore, it appears possible to attain relatively high ionizer temperatures without the usual problems of heater and heater insulator failure.

Engine Design

Three factors dictate the selection of accelerator length. The first is that the length be shorter than the ion cyclotron

radius $L \ll r_i$. The second has been derived previously and states that the length be made as long as possible to decrease J_{ez}. The third arises from consideration of the azimuthal drift motion of electrons v_{eD} through a background of essentially stationary ions. This situation is similar to that of an electron beam moving through a stationary plasma, which can result in the onset of a two-stream instability caused by the growth of electrostatic space-charge waves.

An analysis conducted of the plasma within the low-density Hall accelerator[6] indicates that azimuthal space-charge waves can grow due to a two-stream instability at azimuthal drift velocities ($v_D = E/B$) above a critical value. Experiments in a gas-discharge Hall accelerator[6] have provided evidence to substantiate this theory, and it is to be anticipated that this critical condition will apply equally well to the present device. The principal result is that, at drift velocities above the critical value, periodic azimuthal electric field fluctuations will cause large increases in J_{ez} due to $\mathbf{E}_\theta \times \mathbf{B}_r$ drifts. This critical drift velocity is determined by the ion temperature (in a frame of reference moving at v_i) and electron mass such that

$$v_{eD_{cr}} = E_{cr}/B = (kT_i/m_e)^{1/2} \tag{6}$$

Hence there exists a critical electric field above which electron backflow would be expected to increase markedly. Since $E \approx V_a/L$, for a given applied accelerating voltage it is necessary to increase accelerator length such that $L > V_a/E_{cr}$. Alternately, for design purposes, it is necessary that

$$L > L_{cr} = V_a(m_e/kT_i)^{1/2}/B \tag{7}$$

where the ion temperature is approximately equal to the ionizer temperature in the absence of appreciable volume ionization and electron-ion collisions. The effect of accelerating voltage V_a on accelerator length is depicted in Fig. 6 for various values of B and T_i.

The ion cyclotron radius limit, also shown on Fig. 6, has been selected conservatively in that the accelerator length is approximately an order of magnitude smaller than the radius of a cesium ion moving at an energy eV_a. As indicated in Fig. 6, it is possible to avoid the onset of losses due to both two-stream instabilities and ion swirl at ion energies corresponding to 3000 sec specific impulse and at $T_i = 1600$ K. This can be accomplished with reasonable accelerator lengths (~10 cm) and magnetic fields (~400 gauss).

In order to minimize wall losses it is desirable that the annulus height approximately equal the accelerator length. Hence the present device appears to be most suitable for operation in large sizes and at high over-all thrust and power levels. A lower limit on length, and hence accelerator area and thrust, is established by core saturation at the higher magnetic fields required (Fig. 6).

In view of the many factors potentially capable of affecting the magnitude of electron backflow and hence over-all efficiency, an experimental program was undertaken to provide some preliminary data on the operation of a model accelerator.

Experimental Apparatus

The accelerator is sketched in Fig. 7. The porous ionizer C has a mean diameter of 8.9 cm and a frontal area of 35.5 cm^2. The ionizer vapor duct B is fed from three feed tubes V (see Fig. 8). Heat shields A are used to reduce thermal power losses. The accelerating region is approximately 2.5 cm long. This length was chosen for compatibility with the ionizer size, which was limited by existing porous-tungsten fabrication capability and the desire to avoid development problems at an early stage. These dimensions allowed the test program to be conducted in an available 12-in.-diam vacuum facility. The ionizer heater has required some development work and is presently limited to temperatures of about 1450 K. The heater H is constructed of 30-mil rhenium wire and is supported by an alumina insulator recessed into the ionizer duct. The cathode (neutralizer) E is a directly heated, overwound tantalum filament coated with lanthanum hexaboride and is supported externally in the present design to simplify fabrication and assembly.

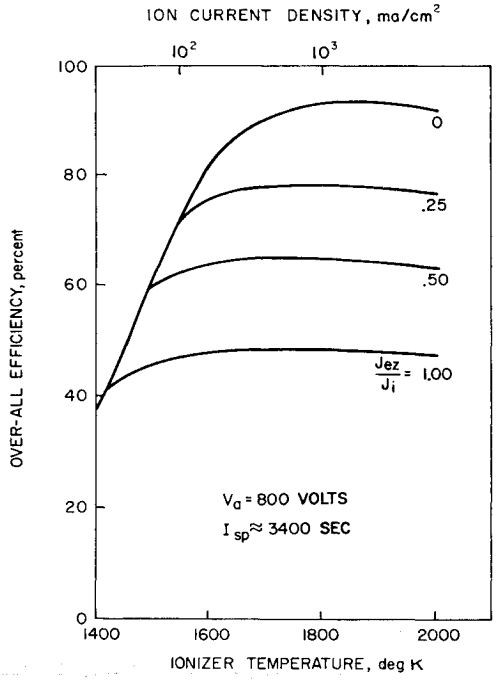

Fig. 5 Effect of electron backflow.

The pole pieces of the ferromagnetic core have been flame-sprayed with alumina to provide the insulating walls depicted in Fig. 1. As shown in Fig. 7, this insulation extends completely over the portions of both pole pieces exposed to cathode electrons. A shield F has been installed to screen the high potential feed system to prevent possible breakdown between the feed system and the cesium plasma. The inner pole piece J has been fabricated from 2V Permendur because of its high induction saturation limit and high Curie temperature. The present design permits operation at fields in excess of 3000 gauss before saturation. A short space-gap L has been left in the inner pole piece to permit measurements of magnetic fields by means of a Hall probe. The probe can be used to detect a decrease in magnetic flux caused by the presence of $J_{e\theta}$ in the accelerating region. The solenoid coil and inner pole piece are water cooled to minimize the effects of temperature variations on the Hall probe reading.

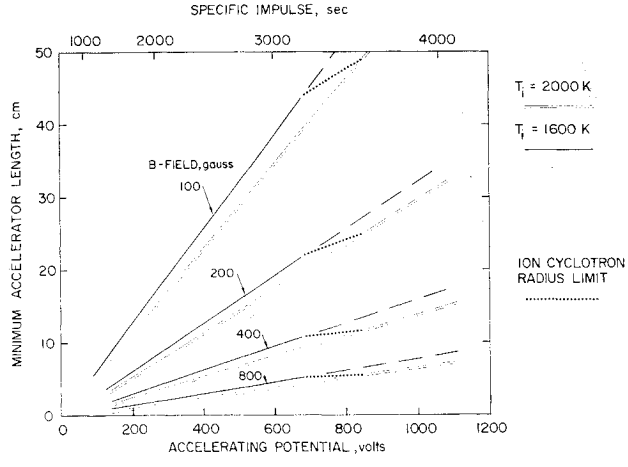

Fig. 6 Effect of stability limit on accelerator length.

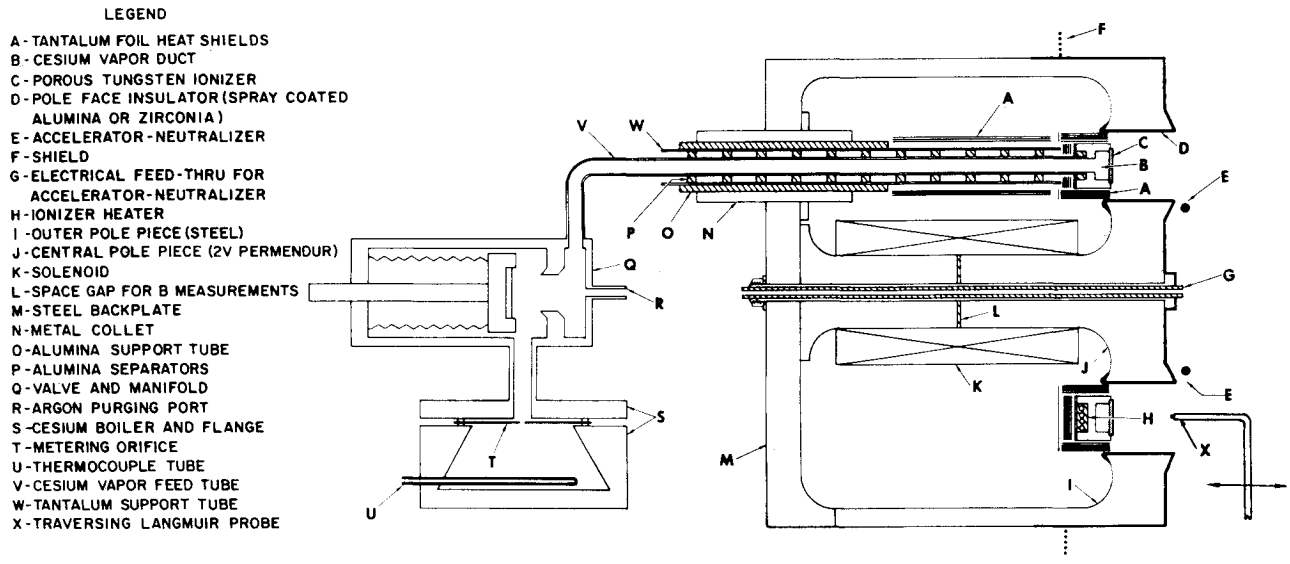

Fig. 7 Schematic diagram of experimental accelerator.

The present cesium feed system consists of an electrically heated boiler, an orifice plate, a shutoff valve, and an argon purging system. All components downstream of the boiler are heated to prevent cesium condensation. The boiler is operated at constant temperature under saturated conditions and is calibrated by flow depletion methods.

To operate the accelerator, the boiler, ionizer, and cathode are raised to operating temperatures and the feed system is allowed to reach equilibrium conditions. With the magnetic field and accelerating voltage applied, current flow may be started and stopped by opening and closing the cesium feed valve (Fig. 7).

The test facility incorporates a cesium condenser which can be cooled with water or LN_2 and a water-cooled, calorimeter target constructed of copper honeycomb. Ambient pressures on the order of 10^{-6} mm Hg can be maintained during operation using a water-baffled, 4-in., oil-diffusion pump. Ionizer temperature is monitored by means of thermocouples and by an optical pyrometer. Voltages, currents, and temperatures are monitored at all significant locations. A traversing device having two degrees of freedom has been provided to conduct measurements with a Langmuir probe X at various axial and radial stations.

Preliminary Experimental Results

At least two different modes have been observed at low cesium flow rates (approximately 0.2 amp of equivalent ion current); a high-voltage, low-current mode, and a low-voltage, high-current mode. The high-voltage mode appears to have the desired characteristics; i.e., an electric field is maintained within the plasma. In the low-voltage mode, the major portion of the applied potential difference apparently occurs across the cathode sheath. The onset of the low-voltage mode at present appears to be a function of V_a, B, and cesium flow rate. At mass flows in excess of 1.0 amp the low-voltage mode does not occur.

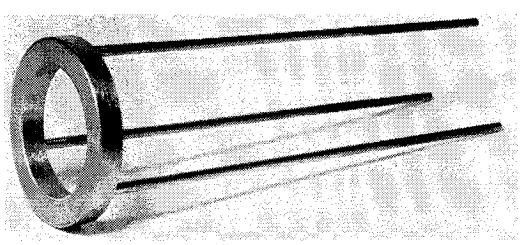

Fig. 8 Porous tungsten ionizer and cesium feed tubes.

In the high-voltage mode, potential differences of up to 400 v have been maintained across the accelerator at magnetic fields of from 20 to 1000 gauss with the accelerator and power supply electrically isolated from the test chamber and target. Under conditions in which the cathode is not emission limited, the cathode potential floats to within a few volts of target potential. Measurements of beam plasma potential indicate that the exhaust beam is nearly at cathode potential during such operation.

Estimates of ion current have been made by biasing the target a few volts negative with respect to the cathode. It has been found that the discharge characteristics do not change appreciably, as the target is biased in this fashion. The data given in Table 1 are representative of results obtained to date. It should be noted that considerable error (up to 25%) may exist in the values quoted for cesium flow rate because of the limitations imposed by the present feed system. Furthermore the target ion current may be somewhat in error as a result of secondary emission, since target suppressor grids have not as yet been employed.

Major questions regarding the origin and kinetic energy of the exhaust beam ions have yet to be answered. The range of the present experiments is shown in Fig. 3. Under these conditions, the largest portion of the target thermal input is due to ionizer radiation. The radiative absorptivity of the present calorimeter target appears to change with varying cesium coverage, although the target face is of honeycomb construction. Accordingly, since the calorimetric target has been proven to be unreliable in determining beam kinetic

Table 1 Typical discharge characteristics

Case →	1	2	3	4	5
Accelerator voltage V_a, v	80	160	100	200	350
Accelerator current I_a, amp	1.05	0.95	2.0	2.2	2.4
Cathode current (floating), amp	1.05	0.95	2.0	2.2	2.4
Cathode current (biased), amp	0.70	0.60	0.70	0.70	0.34
Target ion current I_i, amp	0.29	0.28	1.3	1.5	2.05
Equivalent Cs flow rate, amp	0.20	0.20	1.3	1.3	1.3
Magnetic field, gauss	50	50	610	610	975

power, it has been replaced with a target thrust balance, and measurements are now in progress to determine beam momentum efflux directly.

Measurements have also been made of the axial potential distribution at the mean annulus radius using the traversing Langmuir probe shown in Fig. 7. For $V_a = 150$ v, a drop of 110 v has been observed in a region extending from within 3 mm of the ionizer plane to the cathode plane. The potential has been found to decrease rapidly in the vicinity of the ionizer and more slowly in the vicinity of the cathode. Electron temperatures determined from probe curves have been found to support the hypothesis of adiabatic electron backflow, when compared with local plasma potentials. Measured electron densities agree to within a factor of 2 with ion densities calculated from measured target ion currents and local plasma potentials.

Concluding Discussion

The application of low-density Hall-current acceleration to electrical propulsion has potential advantages in terms of operation at high thrust densities in the intermediate specific impulse regime. Analyses of an accelerator in which ions are formed by surface contact ionization indicate that efficient performance is potentially achievable at high thrust densities, even at relatively high percentages of electron backflow. Under these conditions the major portion of the ionizer power input is derived from electron bombardment, substantially reducing and even eliminating ionizer heater power requirements. Because of the large ionization cross section of cesium, the probability of electron impact ionization in the immediate vicinity of the ionizer is high and the accelerator is quite tolerant of ionizer neutral efflux. (For representative conditions of electron density and energy, the mean free path of a neutral before undergoing ionization is of the order of 0.01 cm.) As ionizer effectiveness decreases, therefore, volume ionization may play an increasingly significant role.

In the experiments performed to date on the present accelerator, operation at current neutralized conditions has been achieved simply by floating the engine and power supply with respect to the test facility. Ion current measurements obtained by biasing the cathode slightly have indicated currents of the same order as the cesium flow rate, and ion current densities in excess of 40 ma/cm^2. These values are considerably in excess of the ion current densities expected from surface contact ionization at the ionizer temperatures employed. However, in tests in which the ionizer temperature is varied by adjusting the heater input power while the accelerator is operating, increments in ion current are observed which are in agreement with porous tungsten ion emission data. These results indicate that volume ionization of cesium neutrals has constituted the major source of ion current at the higher mass flow rates. The question whether ions formed in the accelerating region are accelerated through the full applied voltage has yet to be answered. It is anticipated that planned thrust target measurements will resolve this point. Should the majority of ions be formed at nearly anode potential, it would indicate that efficient thrustor operation is achievable with a cesium gas-discharge Hall accelerator. The large ionization cross section[10] and low ionization potential of cesium suggests that it may be quite attractive for use as a propellant in such a thrustor. (Hall accelerator operation could not be achieved with argon in the configuration shown in Fig. 7 under any conditions of mass flow and ambient pressure.)

From the measured target current data it appears that the impedance of the discharge to axial electron currents is sufficiently high to reduce electron backflow to values below the ion current under conditions in which the magnetic field is sufficiently large to avoid the two-stream instability limit. For conditions under which two-stream instabilities would be expected to occur, the backflow is about twice the target current.

While over-all performance data on low-density Hall-current accelerator operations are not yet available, preliminary tests of a model accelerator have indicated that some conditions essential to proper performance have been met. Work is presently in progress to determine experimentally those factors necessary for a more complete evaluation.

References

[1] Lary, E. C., "Ion acceleration in a space-charge neutral plasma," UAC Research Lab. Rept. UAR-A125 (June 1962).

[2] Seikel, G. R. and Reshotko, E., "Hall current ion accelerator," Bull. Am. Phys. Soc. **7**, 414 (1962).

[3] Lary, E. C., Meyerand, R. G., Jr., and Salz, F., "Ion acceleration in a gyro-dominated neutral plasma theory and experiment," Bull. Am. Phys. Soc. **7**, 441 (1962).

[4] Janes, G. S., Dotson, J., and Wilson, T., "Electrostatic acceleration of neutral plasmas—momentum transfer through magnetic fields," *Proceedings of the Third Symposium on Advanced Propulsion Concepts* (U. S. Air Force, Office of Scientific Research, Cincinnati, Ohio, October 1962).

[5] Hess, R. V., "Fundamentals of plasma interaction with electric and magnetic fields," NASA SP-25, pp. 9–32 (1963).

[6] Lary, E. C., Meyerand, R. G., Jr., and Salz, F., "Fluctuations in a gyro-dominated plasma," *Comptes Rendus de la VI Conférence Internationale sur les Phénomènes d'Ionisation dans les Gaz* (S.E.R.M.A., Paris, France, 1963), Vol. II, Sec. VC, p. 441.

[7] Hoh, F. C., "Low-temperature plasma diffusion in a magnetic field," Rev. Mod. Phys. **34**, 267–286 (1962).

[8] Taylor, J. B. and Langmuir, I., "The evaporation of atoms, ions and electrons from cesium films on tungsten," Phys. Rev. **44**, 423–458 (1933).

[9] Husmann, O. K., "A comparison of the contact ionization of cesium on tungsten with that of molybdenum, tantalum, and rhenium surfaces," AIAA J. **1**, 2607–2614 (1963).

[10] Baker, F. S. and Brink, G. O., "The ionization of alkali atoms by electron bombardment," Univ. of Calif., Livermore, UCRL-7087 (October 1962).